

Exponential Step Sizes for Non-Convex SGD

Xiaoyu Li*
Boston University
xiaoyuli@bu.edu

Zhenxun Zhuang*
Boston University
zxzhuang@bu.edu

Francesco Orabona
Boston University
francesco@orabona.com

Abstract

Stochastic Gradient Descent (SGD) is a popular tool in training large-scale machine learning models. Its performance, however, is highly variable, depending crucially on the choice of the step sizes. Accordingly, a variety of strategies on tuning the step sizes have been proposed. Yet, most of them lack a theoretical guarantee, whereas those backed by theories often do not shine in practice. Regarding this, we introduce the exponential step sizes, a novel strategy that is simple to use and enjoys both theoretical and empirical support. In particular, we prove its almost optimal convergence rate for stochastic optimization of smooth non-convex functions. Furthermore, in the case where the PL condition holds, this strategy can automatically adapt to the level of noise without knowing it. Finally, we empirically verified on real-world datasets with deep learning architectures that, requiring only two hyperparameters to tune, it bests or matches the performance of various finely-tuned state-of-the-art strategies including Adam and cosine decay.

1 Introduction

In the last 10 years, non-convex machine learning formulations have received more and more attention as they can typically better scale with the complexity of the predictors and the amount of training data compared with convex formulations. One such example is the deep neural networks. Over the years, various algorithms have been proposed and employed to optimize non-convex machine learning problems, among which Stochastic Gradient Descent (SGD) [Robbins and Monro, 1951] has become the most important ingredient in Machine Learning pipelines. Practitioners prefer it over more sophisticated methods for its simplicity and speed. Yet, this generality comes with a cost: SGD is far from the robustness of, e.g., second-order methods that require little to no tweaking of knobs to work. In particular, the step size is still the most important parameter to tune in the SGD algorithm, carrying the actual weight of making SGD adaptive to different situations.

The importance of step sizes in SGD is testified by the large number of proposed strategies to tune step sizes, backed by theory and/or empirical evidence [Duchi et al., 2010, McMahan and Streeter, 2010, Tieleman and Hinton, 2012, Zeiler, 2012, Kingma and Ba, 2015]. The most successful ones in empirical trials are the *stagewise step decay* [Krizhevsky et al., 2012, Simonyan and Zisserman, 2015, He et al., 2016, Huang et al., 2017] and the *cosine decay* [Loshchilov and Hutter, 2017, He et al., 2019]. The stagewise step decay starts the training with a relatively large constant step size, and then periodically decreases the step size, for example when the curve of the validation loss plateaus. Indeed, assuming we were able to know in advance the unknown quantities of the function to be optimized, it can also be shown that the stagewise step decay would be theoretically optimal Hazan and Kale [2011]. However, in practice, we typically do not have access to those quantities about the function so the tuning can become hard. On the other hand, the other most frequently used step size schedule, the cosine decay, is simple to use requiring only one hyperparameter, but it is only a heuristic without a theoretical justification.

In this paper, we overcome the above issues by proposing the use of *exponentially decaying step sizes*, which is at the same time *simple to use and backed by both theory and empirical effectivity*.

Specifically, the contributions of this paper are as follows:

- We show that SGD with exponentially decaying step sizes has an optimal convergence rate for smooth non-convex functions, matching the one of polynomial step sizes up to poly-logarithmic terms,

*The first two authors contributed equally to this work.

- In the case when the function also satisfies the Polyak-Lojasiewicz (PL) condition [Polyak, 1963, Lojasiewicz, 1963, Karimi et al., 2016], this step size strategy automatically adapts to the level of noise in the gradients. This rate is new in the literature for PL functions.
- We validate our theory with experiments on deep learning architectures: Exponential step sizes have essentially matching or better empirical performance than polynomial step decay, stagewise step decay, cosine decay, and Adam [Kingma and Ba, 2015], while requiring only two hyperparameters.

The rest of the paper is organized as follows: We first discuss the relevant literature (Section 2). In Section 3, we introduce the notation, setting, and precise assumptions. Then, in Section 4 we describe in detail the step sizes and the theoretical guarantees. We show our empirical results in Section 5. Finally, we conclude with a discussion of the results and future work.

2 Related Work

Nonconvex optimization with the PL condition. We pay special attention to the PL condition in that it has been shown to hold in many important non-convex problems in machine learning. Karimi et al. [2016] show that for a smooth function, strong convexity and Restricted Secant Inequality (RSI) [Zhang and Yin, 2013] are both special cases of PL. On the other hand, the two forms of one-point convexity summarized in [Zhu, 2018b] are special cases of RSI and PL, respectively, thus in turn imply the PL condition. Hence, two-layer neural networks [Li and Yuan, 2017], dictionary learning [Arora et al., 2015], phase retrieval [Chen and Candes, 2015], and matrix completion [Sun and Luo, 2016], which all satisfy the one-point convexity [Zhu, 2018b], all satisfy the PL condition. Furthermore, Kleinberg et al. [2018] empirically observed that the loss surface of neural networks has good one-point convexity properties, and thus locally satisfies the PL condition. Stochastic optimization algorithms under the PL condition have been widely studied. For classic SGD, Karimi et al. [2016] proved the rate of $O(1/\mu^2T)$ for SGD with polynomial step sizes assuming Lipschitz and smoothness, where μ is the PL constant. Note that the Lipschitz assumption is not necessary to achieve the same rate, see Theorem 3 in the Appendix. Considering functions with finite-sum structure, Reddi et al. [2016] and Lei et al. [2017] proved improved rates for variance reduction methods. However, the result is not true for the classic SGD and it might be important to note that variance reduction methods seem to have problems in deep learning applications [Defazio and Bottou, 2019]. As far as we know, $O(1/\mu^2T)$ is the best-known rate for non-convex SGD under the PL condition and we match it in Theorem 1.

Stagewise step decay. To the best of our knowledge, the exponential step size we propose has never been analyzed in the literature.¹ The closest strategy is the *stagewise step decay*, which corresponds to the discrete version of the exponential step size we analyze. This strategy is known with many different names: “stagewise step size” [Yuan et al., 2019], “step decay schedule” [Ge et al., 2019], “geometrically decaying schedule” [Davis et al., 2019b], and “geometric step decay” [Davis et al., 2019a]. In this paper, we will call it stagewise step decay. This approach was first introduced in [Goffin, 1977]. In the stochastic convex optimization literature, this decay strategy was first used by [Hazan and Kale, 2011] to remove logarithmic factors in the stochastic optimization of strongly convex functions. Recently, this decay strategy has been used to achieve improved rates of convergence for stochastic minimization of strongly convex functions [Aybat et al., 2019, Kulunchakov and Mairal, 2019], in accelerated stochastic subgradient methods for convex functions which satisfy local growth condition [Xu et al., 2016], and for the stochastic minimization of quadratic functions [Ge et al., 2019]. Interestingly, Ge et al. [2019] also show promising empirical results on non-convex functions, but instead of using their proposed decay strategy, they use an exponentially decaying schedule, like the one we analyze here. However, all these works focus on the convex settings, where the achievable rates are better than in the PL one, see Section 4.2 (Optimality of the bounds). The exceptions are the use in non-convex sharp [Davis et al., 2019a] and weakly-quasi-convex functions [Yuan et al., 2019], which are not comparable with PL functions.

Step size strategies for SGD. Besides the stagewise step decay, there are other interesting strategies proposed for the step sizes of SGD. Vaswani et al. [2019b] considers a line-search technique to set the step sizes in SGD, for convex and non-convex functions satisfying the strong growth condition. However, their

¹Despite the name, the exponential step size has no relationship with the one in Li and Arora [2020], where an exponentially *increasing* step size is analyzed under very special conditions.

analysis requires a finite-sum structure of the objective function and the strong growth condition implies that we are in the interpolation regime. On the contrary, we do not assume finite-sum structure, but we use the assumption $\mathbb{E}_t \|\nabla f(\mathbf{x}_t) - \mathbf{g}_t\|^2 \leq a \|\nabla f(\mathbf{x}_t)\|^2 + b$. It tells that the variance of the noise is upper bounded by the squared gradient norm and an additional constant. This actually covers the expected strong growth condition (by setting $b = 0$) in [Khaled and Richtárik \[2020\]](#). Cosine decay has been studied in [Loshchilov and Hutter \[2017\]](#) and [He et al. \[2019\]](#), but only empirically.

3 Problem Set-up

Notation. We denote vectors by bold letters, e.g. $\mathbf{x} \in \mathbb{R}^d$. We denote by $\mathbb{E}[\cdot]$ the expectation with respect to the underlying probability space and by $\mathbb{E}_t[\cdot]$ the conditional expectation with respect to the past. Any norm in this work is the ℓ_2 norm.

Setting and Assumptions. We consider the unconstrained optimization problem $\min_{\mathbf{x} \in \mathbb{R}^d} f(\mathbf{x})$, where $f(\mathbf{x}) : \mathbb{R}^d \rightarrow \mathbb{R}$ is a function bounded from below and we denote its infimum by f^* . Note that we do not require f to be convex.

We focus on SGD, where, after an initialization of the first iterate as any $\mathbf{x}_1 \in \mathbb{R}^d$, in each round $t = 1, 2, \dots, T$ we receive \mathbf{g}_t , an unbiased estimate of the gradient of f at point \mathbf{x}_t , i.e., $\mathbb{E}_t \mathbf{g}_t = \nabla f(\mathbf{x}_t)$. We update \mathbf{x}_t with a step size η_t , i.e., $\mathbf{x}_{t+1} = \mathbf{x}_t - \eta_t \mathbf{g}_t$.

We also assume that

(A1) f is L -smooth, that is, f is differentiable and its gradient $\nabla f(\cdot)$ is L -Lipschitz, namely $\|\nabla f(\mathbf{x}) - \nabla f(\mathbf{y})\| \leq L \|\mathbf{x} - \mathbf{y}\|, \forall \mathbf{x}, \mathbf{y} \in \mathbb{R}^d$. This assumption implies [\[Nesterov, 2004, Lemma 1.2.3\]](#)

$$|f(\mathbf{y}) - f(\mathbf{x}) - \langle \nabla f(\mathbf{x}), \mathbf{y} - \mathbf{x} \rangle| \leq \frac{L}{2} \|\mathbf{y} - \mathbf{x}\|^2, \quad \forall \mathbf{x}, \mathbf{y} \in \mathbb{R}^d. \quad (1)$$

(A2) f satisfies the μ -PL condition, that is, for some $\mu > 0$, $\frac{1}{2} \|\nabla f(\mathbf{x})\|^2 \geq \mu (f(\mathbf{x}) - f^*)$, $\forall \mathbf{x}$.

In words, the gradient grows at least as the square root of the sub-optimality.

(A3) For $t = 1, 2, \dots, T$, we assume $\mathbb{E}_t[\|\mathbf{g}_t - \nabla f(\mathbf{x}_t)\|^2] \leq a \|\nabla f(\mathbf{x}_t)\|^2 + b$, where $a, b \geq 0$.

Note that this is more general than the common assumption of assuming a bounded variance, i.e., $\mathbb{E}_t[\|\mathbf{g}_t - \nabla f(\mathbf{x}_t)\|^2] \leq \sigma^2$. Indeed, our assumption recovers the bounded variance case with $a = 0$ while also allowing for the variance to grow unboundedly far from the optimum when $a > 0$. This relaxed assumption on the noise was first used by [Bertsekas and Tsitsiklis \[1996\]](#) (see Proposition 4.2) to prove the asymptotic convergence of SGD.

4 Exponential Step Sizes

In this section, we present the details of the novel exponential step sizes and the analysis of SGD on the non-convex smooth functions with this step size strategy.

4.1 Motivation

For the stochastic optimization of smooth functions satisfying the PL condition, the optimal step sizes must be chosen in a way that is very dependent on the noise: In the noise-free case, a constant step size is used to get a linear rate, while in the noisy case the best rate $O(1/T)$ is given by time-varying step sizes $O(1/\mu t)$ [\[Karimi et al., 2016\]](#). Similarly, without the PL condition, we still need a constant step size in the noise-free case and a $O(\frac{1}{\sqrt{t}})$ step size in the noisy case [\[Ghadimi and Lan, 2013\]](#). In practice, this means that each noise level, i.e., mini-batch size, needs a different step size.

Another possibility is to use the stagewise step decay. For example, [Ge et al. \[2019\]](#) propose to start from a constant step size and cut it by a fixed factor every $O(\ln T)$ steps, decaying coarsely to $O(1/T)$ after T iterations. However, in practice the choice of when to cut the step size becomes a series of hyperparameters to tune, making this strategy difficult to use in real-world applications.

Instead of using the stagewise step decay in a discrete way, one might think of doing it in a *continuous fashion*. Therefore, here we consider the following exponential step sizes:

$$\eta_t = \eta_0 \cdot \alpha^t, \quad (2)$$

where $\alpha = (\beta/T)^{1/T}$, $\beta \geq 1$, $\eta_0 \leq (L(1+a))^{-1}$, and a and L are defined in **(A1, A3)**.

Let's see how the exponential step size evolves. First, we can expect that, in the early stage of the optimization process, the disturbance due to the noise is relatively small compared to how far we are from the optimal solution. Accordingly, at this phase, η_t is not far away from η_0 which is the step size we would use in the noiseless case. On the other hand, when the iterate is close to the optimal solution, we have to decrease the step size to fight with the effect of the noise. In this stage, η_t converges to $O(1/T)$, which is the optimal step size used in the noisy case. Overall, *the exponential step size is emulating the transition between the optimal constant one at the beginning and the decreasing one towards the end in a smooth continuous way.*

Next, we formalize these intuitions showing that the exponential step size works in any noise condition under the PL case, while still guarantees convergence to a stationary point without the PL condition.

4.2 Convergence Guarantees

We now prove the convergence guarantees for the exponential step size.

First, we consider the case where the function is smooth and satisfies the PL condition.

Theorem 1. *Assume **(A1, A2, A3)**. For a given $T \geq \max\{3, \beta\}$ and $\eta_0 = (L(1+a))^{-1}$, with step size (2), SGD guarantees*

$$\mathbb{E}f(\mathbf{x}_{T+1}) - f^* \leq \frac{5LC(\beta)}{e^2\mu^2} \frac{\ln^2 \frac{T}{\beta}}{T} b + C(\beta) \exp\left(-\frac{0.69\mu}{L+a} \left(\frac{T}{\ln \frac{T}{\beta}}\right)\right) \cdot (f(\mathbf{x}_1) - f^*),$$

where $C(\beta) \triangleq \exp\left(\frac{2\mu\beta}{L(1+a)\ln \frac{T}{\beta}}\right)$.

Adaptivity to Noise. The exponential step size is adaptive to the noise: the *same step size* gives a linear rate when $b = 0$, while recovers the order of $O(1/T)$ when $b \neq 0$ (up to poly-logarithmic terms). In contrast, polynomial step sizes would require two different settings—decaying vs constant—in the noisy vs no-noise situation. This rate is new in the literature on PL functions. It is possible to obtain similar but incomparable rates for strongly convex and smooth functions [Zhu, 2018a, Aybat et al., 2019], but here we do not need convexity.

Choice of β . Note that if $\beta = L(1+a)/\mu$, we get the bound

$$\mathbb{E}f(\mathbf{x}_{T+1}) - f^* \leq \frac{5L}{\mu^2} \frac{\ln^2 \frac{\mu T}{L}}{T} b + e^2 \exp\left(-\frac{0.69\mu}{L+a} \left(\frac{T}{\ln \frac{\mu T}{L}}\right)\right) \cdot (f(\mathbf{x}_1) - f^*).$$

In words, this means that we are basically free to choose β , but will pay an exponential factor in the mismatch between β and $\frac{L}{\mu}$, which is basically the condition number for PL functions. This is similar to what happens in the stochastic optimization of strongly convex functions [Bach and Moulines, 2011].

Optimality of the bounds. As far as we know, no lower bound is known for the stochastic optimization of non-convex smooth functions under the PL condition. However, up to poly-logarithmic terms, Theorem 1 matches at the same time the best-known rates for the noisy and deterministic cases [Karimi et al., 2016] (see also Theorem 3 in the Appendix). Note that this rate is not comparable with the one for strongly convex functions that is $O(1/\mu T)$.

Convergence without the PL condition. The PL condition tells us that all stationary points are optimal points [Karimi et al., 2016], which is not always true for the parameter space in deep learning [Jin et al., 2017]. However, this condition might still hold locally, for a considerable area around the local minimum. The previous theorem tells us that once we reach the area where the geometry of the objective function satisfies the PL condition, we can get to the optimal point with an almost linear rate, depending on the noise. However, we still have to be able to reach that region. Hence, in the following, we discuss the case where the PL condition is not satisfied and show that the exponential step sizes are still able to move to a critical point at the optimal speed.

Theorem 2. Assume **(A1)**, **(A3)** and $c > 1$. SGD with step sizes (2) with $\eta_0 = (cL(1+a))^{-1}$ guarantees

$$\mathbb{E}\|\nabla f(\tilde{\mathbf{x}}_T)\|^2 \leq \frac{bT}{c(a+1)(T-\beta)} + \frac{3Lc(a+1)\ln\frac{T}{\beta}}{T-\beta} \cdot (f(\mathbf{x}_1) - f^*),$$

where $\tilde{\mathbf{x}}_T$ is a random iterate drawn from $\mathbf{x}_1, \dots, \mathbf{x}_T$ with $\mathbb{P}[\tilde{\mathbf{x}}_T = \mathbf{x}_t] = \frac{\eta_t}{\sum_{i=1}^T \eta_i}$.

If $b \neq 0$ in **(A3)**, setting $c \propto \sqrt{T}$ and $\beta = O(1)$ would give the optimal $\tilde{O}(\frac{1}{\sqrt{T}})$ rate; whereas if $b = 0$, setting $c = O(1)$ and $\beta = O(1)$ yields a $\tilde{O}(\frac{1}{T})$ rate. Hence, the exponential step size in this setting is basically as powerful as the polynomial ones. It is worth noting that the condition $b = 0$ holds in many practical scenarios [Vaswani et al., 2019a].

Proofs of the Theorems. Before proving our results, we introduce some technical lemmas whose proofs are in the Appendix.

Lemma 1. Assume $X_k, A_k, B_k \geq 0, k = 1, \dots$, and $X_{k+1} \leq A_k X_k + B_k$, then we have

$$X_{k+1} \leq \prod_{i=1}^k A_i X_1 + \sum_{i=1}^k \prod_{j=i+1}^k A_j B_i.$$

Lemma 2. $\exp\left(\frac{\mu\alpha^{T+1}}{L(1+a)(1-\alpha)}\right) \leq C(\beta)$, where $C(\beta)$ is defined in Theorem 1.

Lemma 3. $1 - x \leq \ln\left(\frac{1}{x}\right), \forall x > 0$.

We can now prove the theorems.

Proof of Theorem 1. For simplicity, denote $\mathbb{E}f(\mathbf{x}_t) - f^*$ by Δ_t . By (1), we have

$$f(\mathbf{x}_{t+1}) \leq f(\mathbf{x}_t) - \langle \nabla f(\mathbf{x}_t), \eta_t \mathbf{g}_t \rangle + \frac{L}{2} \eta_t^2 \|\mathbf{g}_t\|^2.$$

Taking expectation on both sides and using the PL-condition, we get

$$\begin{aligned} \Delta_{t+1} - \Delta_t &\leq -\eta_t \mathbb{E}\|\nabla f(\mathbf{x}_t)\|^2 + \frac{L}{2} \eta_t^2 (\mathbb{E}\|\nabla f(\mathbf{x}_t)\|^2 + \mathbb{E}\|\mathbf{g}_t - \nabla f(\mathbf{x}_t)\|^2) \\ &\leq -\eta_t \mathbb{E}\|\nabla f(\mathbf{x}_t)\|^2 + \frac{L(a+1)}{2} \eta_t^2 \mathbb{E}\|\nabla f(\mathbf{x}_t)\|^2 + \frac{L}{2} \eta_t^2 b \\ &\leq -(2\mu\eta_t - \mu L(1+a)\eta_t^2) \Delta_t + \frac{L}{2} \eta_t^2 b \leq -\mu\eta_t \Delta_t + \frac{L}{2} \eta_t^2 b, \end{aligned}$$

where in the last inequality we used the fact that $\eta_t \leq \frac{1}{L(1+a)}$.

Rearranging, we have $\Delta_{t+1} \leq (1 - \mu\eta_t) \Delta_t + \frac{L}{2} \eta_t^2 b$. Then, by Lemma 1, we have

$$\begin{aligned} \Delta_{T+1} &\leq \frac{L}{2} \sum_{t=1}^T \prod_{i=t+1}^T \left(1 - \frac{\mu\alpha^i}{L(1+a)}\right) \frac{\alpha^{2t}}{L^2(1+a)^2} b + \prod_{t=1}^T \left(1 - \frac{\mu\alpha^t}{L(1+a)}\right) \Delta_1 \\ &\leq \frac{b}{2L(1+a)^2} \sum_{t=1}^T \exp\left(-\frac{\mu}{L(1+a)} \sum_{i=t+1}^T \alpha^i\right) \alpha^{2t} + \exp\left(-\frac{\mu}{L(1+a)} \sum_{t=1}^T \alpha^t\right) \Delta_1 \\ &= \frac{b}{2L(1+a)^2} \sum_{t=1}^T \exp\left(-\frac{\mu(\alpha^{t+1} - \alpha^{T+1})}{L(1+a)(1-\alpha)}\right) \alpha^{2t} + \exp\left(-\frac{\mu(\alpha - \alpha^{T+1})}{L(1+a)(1-\alpha)}\right) \Delta_1, \end{aligned}$$

where in the last inequality we used $1 - x \leq \exp(-x)$.

Using Lemma 2, we obtain

$$\Delta_{T+1} \leq \frac{C(\beta)b}{2L(1+a)^2} \sum_{t=1}^T \exp\left(-\frac{\mu\alpha^{t+1}}{L(1+a)(1-\alpha)}\right) \alpha^{2t} + C(\beta) \exp\left(-\frac{\mu\alpha}{L(1+a)(1-\alpha)}\right) \Delta_1.$$

Using the fact that $\alpha = \left(\frac{\beta}{T}\right)^{\frac{1}{T}} \geq \left(\frac{1}{T}\right)^{\frac{1}{T}} \geq 0.69$ for $T \geq 3$ and Lemma 3, we have

$$\exp\left(-\frac{0.69\mu}{L(1+a)(1-\alpha)}\right) \leq \exp\left(-\frac{0.69\mu}{L(1+a)(1-\alpha)}\right) \leq \exp\left(-\frac{0.69\mu}{L(1+a)} \frac{1}{\ln\left(\frac{1}{\alpha}\right)}\right).$$

Now, using $\exp(-x) \leq \left(\frac{\gamma}{ex}\right)^\gamma, \forall x > 0, \gamma > 0$, we have

$$\begin{aligned} \sum_{t=1}^T \exp\left(-\frac{\mu\alpha^{t+1}}{L(1+a)(1-\alpha)}\right) \alpha^{2t} &\leq \sum_{t=1}^T \left(\frac{e}{2} \frac{\mu\alpha^{t+1}}{L(1+a)(1-\alpha)}\right)^{-2} \alpha^{2t} \\ &\leq \frac{4L^2(1+a)^2}{e^2\mu^2} \sum_{t=1}^T \frac{1}{\alpha^2} \ln^2\left(\frac{1}{\alpha}\right) \leq \frac{10L^2(1+a)^2 \ln^2\frac{T}{\beta}}{e^2\mu^2 T}. \end{aligned}$$

Putting everything together, we get the stated bound. \square

Proof of Theorem 2. Reasoning as in the proof of Theorem 1, we have

$$\begin{aligned} \mathbb{E}f(\mathbf{x}_{t+1}) &\leq \mathbb{E}f(\mathbf{x}_t) - \left(\eta_t - \frac{L(a+1)}{2}\eta_t^2\right) \mathbb{E}\|\nabla f(\mathbf{x}_t)\|^2 + \frac{L}{2}\eta_t^2 b \\ &\leq \mathbb{E}f(\mathbf{x}_t) - \frac{1}{2}\eta_t \mathbb{E}\|\nabla f(\mathbf{x}_t)\|^2 + \frac{L}{2}\eta_t^2 b. \end{aligned} \tag{3}$$

We also observe that

$$\sum_{t=1}^T \eta_t = \frac{\alpha - \alpha^{T+1}}{Lc(a+1)(1-\alpha)} \geq \frac{0.69(1-\alpha^T)}{Lc(a+1)\ln\frac{1}{\alpha}}, \quad \text{and} \quad \sum_{t=1}^T \eta_t^2 \leq \frac{\alpha^2}{L^2c^2(a+1)^2(1-\alpha^2)}.$$

Summing (3) over $t = 1, \dots, T$ and dividing both sides by $\sum_{t=1}^T \eta_t$, we get the stated bound. \square

5 Empirical Results

In this section, we demonstrate the effectivity of our exponential step size compared with other strategies through empirical experiments on using deep neural networks on image classification tasks. Additional experiments in the Appendix: a synthetic one showing in details the noise adaptation, and a NLP one showing a similar pattern of the comparison but on a different task. Codes can be found here.²

Datasets. We consider the image classification task on FashionMNIST and CIFAR-10/100 datasets. For all datasets, we randomly select 10% training images as the validation set. Data augmentation and normalization are described in the Appendix.

Models. For FashionMNIST, we use a CNN model consisting of two alternating stages of 5×5 convolutional filters and 2×2 max-pooling followed by one fully connected layer of 1024 units. To reduce overfitting, 50% dropout noise is used during training. For the CIFAR-10 dataset, we employ the 20-layer Residual Network model [He et al., 2016]; and for CIFAR-100, we utilize the DenseNet-BC model [Huang et al., 2017] with 100 layers and a growth-rate of 12. The loss is cross-entropy. The codes for implementing the latter two models can be found here³ and here⁴ respectively.

Training. During the validation stage, we tune each method using the grid search (full details in the Appendix) to select the hyperparameters that work best according to their respective performance on the validation set. At the testing stage, the best performing hyperparameters from the validation stage are employed to train the model over all training images. The testing stage is repeated with random seeds for 5 times to eliminate the influence of stochasticity.

We use Nesterov momentum [Nesterov, 1983] of 0.9 without dampening (if having this option), weight-decay of 0.0001 (FashionMNIST and CIFAR-10) and 0.0005 (CIFAR100), and use a batch-size of 128.

²<https://github.com/zhenxun-zhuang/SGD-Exponential-Stepsize>

³https://github.com/akamaster/pytorch_resnet_cifar10

⁴<https://github.com/bearpaw/pytorch-classification>

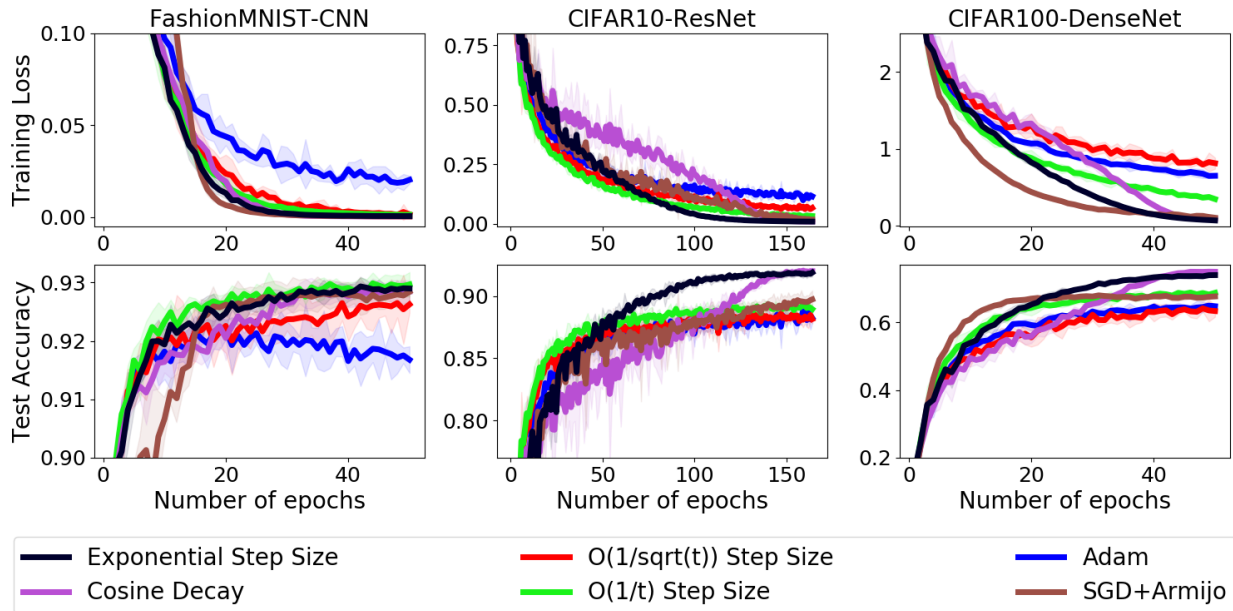


Figure 1: Training loss (top plots) and test accuracy (bottom plots) curves on employing different step size schedules to do image classification using a simple CNN for FashionMNIST (left), a 20-layer ResNet for CIFAR-10 (middle), and a 100-layer DenseNet on CIFAR-100 (right).

Optimization methods. We consider SGD with the following step size decay schedules:

$$\eta_t = \eta_0 \cdot \alpha^t; \quad \eta_t = \eta_0(1 + \alpha\sqrt{t})^{-1}; \quad \eta_t = \eta_0(1 + \alpha t)^{-1}; \quad \eta_t = \eta_0/2(1 + \cos(t\pi/T)), \quad (4)$$

where t is the iteration number (instead of the number of epochs) and the last schedule is the cosine decay [He et al., 2019]. In addition, we also compare with Adam [Kingma and Ba, 2015], SGD+Armijo [Vaswani et al., 2019b], PyTorch’s ReduceLRonPlateau scheduler⁵ and stagewise step decay. In the following, we will call the place of decreasing the step size in stagewise step decay a **milestone**. (As a side note, since we use Nesterov’s accelerated momentum in all SGD variants, the stagewise step decay basically covered the performance of multistage accelerated algorithms [e.g., Aybat et al., 2019].)

Results and discussions. The comparison of performance between our exponential step size and other schemes listed in (4), Adam, and SGD+Armijo are illustrated in Figure 1. More details on the results are available in the Appendix. First of all, the *only* two methods that perform well on *all* 3 datasets are Cosine decay and our exponential step size. In particular, Cosine decay performs the best across datasets, but we can always match their performance both in training loss and test accuracy (except the test accuracy on CIFAR100 where we are slightly behind but far better than others). Despite its great empirical advantage, however, the cosine decay remains a heuristic technique without theoretical justification; in contrast, our method is *backed by firm theoretical guarantees*. Moreover, compared with cosine decay, our decay schedule converges much faster.

On the other hand, as we noted above, stagewise SGD is a very popular decay schedule in deep learning, and Ge et al. [Ge et al. 2019] recently proved its advantage over any polynomial decay schedule. Therefore, to complete the picture, in Figure 2 we compare our decay schedule with stagewise step decay, and ReduceLRonPlateau. The results show that only stagewise step decay with 2 milestones is good in all 3 datasets. However, we can still match the best of them with a fraction of their needed time to find the best hyperparameters. In particular, we need 4 hyperparameters for two milestones, 3 for one milestone, and at least 4 for ReduceLRonPlateau.

Moreover, while it is reasonable to expect that adding even more milestones at the appropriate times could lead to better performance, this would result in a linear growth of the number of hyperparameters

⁵<https://pytorch.org/docs/stable/optim.html>

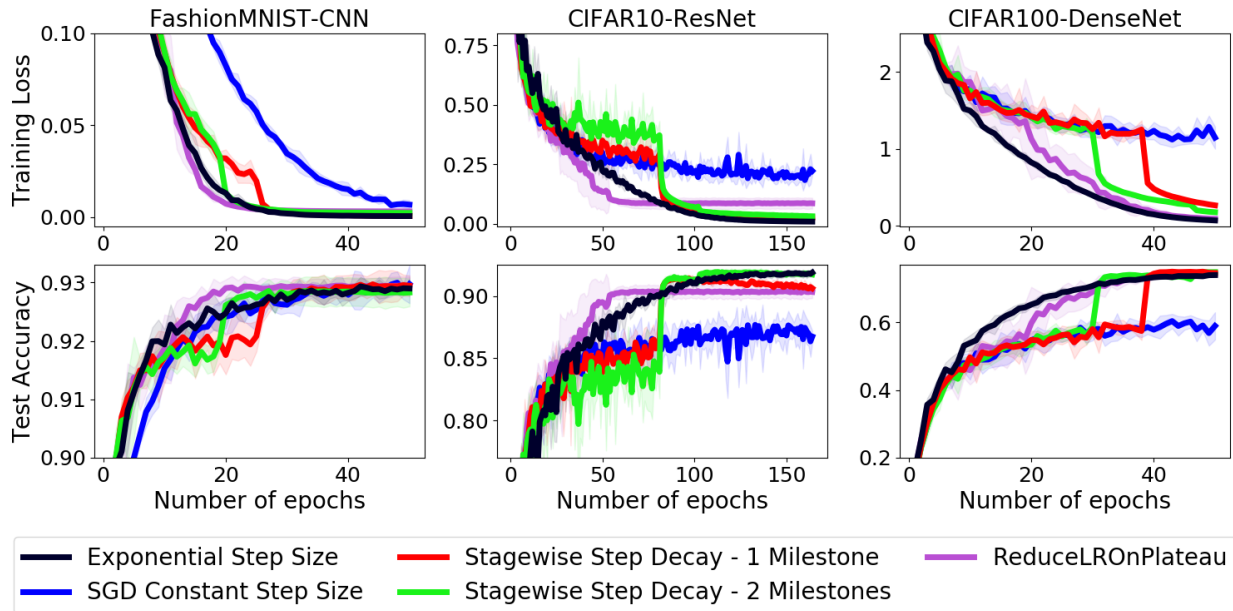


Figure 2: Training loss (top plots) and test accuracy (bottom plots) curves comparing the exponential step size with stagewise step decay for image classification using a simple CNN for FashionMNIST (left), a 20-layer ResNet for CIFAR-10 (middle), and a 100-layer DenseNet on CIFAR-100 (right).

that corresponds to an exponential growth in the tuning time. On the other hand, our decay schedule *only requires 2 hyperparameters* and still gets essentially the best performance.

Note that we do not pretend that our benchmark of the stagewise step decay is exhaustive. Indeed, there are many unexplored (potentially infinite!) possible hyperparameter settings like adding more milestones at carefully chosen locations. However, as one tries to add more and more milestones, the number of possible location combinations will quickly explode, which renders selecting a good set of milestones very hard in practice. Worse still, even the intuition that one should decrease the step size once the test loss curve stops decreasing is not always correct. Indeed, we have observed in experiments (see Figure 3) that after the initial drop of the curve in response to the step size decrease, the test loss curve can gradually go up again.

With that said, we would like to point out the connection between our exponential step size, stagewise step decay, and cosine decay. As we said, the exponential step size can be seen as the continuous form of the stagewise step decay when the number of milestones goes to infinity, see Figure 4. Considering that we can match the empirical performance of the finely tuned stagewise step decay, we have basically provided a “continual” version of it which requires much less tuning efforts. As for the cosine decay, Figure 1 shows that cosine decay progresses very slowly until the latter half of the training process from where on it soon catches up and eventually surpasses other methods. This suggests that the cosine decay scheme of when t is in $[T/2, T]$ plays a central role in its good performance. Again, Figure 4 shows that our exponential step size can approximate the latter half of the cosine decay curve very nicely. As our scheme is backed by theoretical guarantees under the PL condition (see Theorem 1), and as Kleinberg et al. [2018] empirically observes that the loss surface of neural networks enjoys PL condition locally, this work points out a potential direction towards explaining why cosine decay works so well in deep learning.

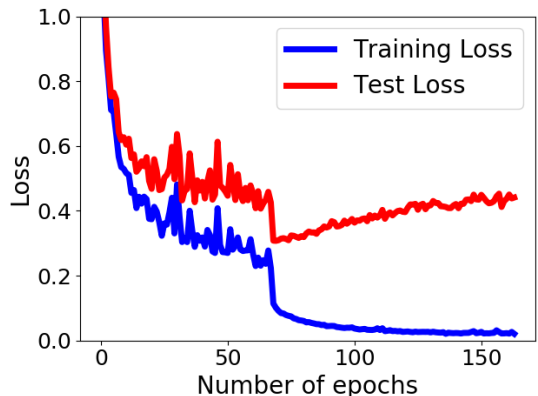


Figure 3: Plot showing that decreasing the step size too soon would lead to overfitting (ResNet20 on CIFAR10).

6 Discussion and Future Work

We have analyzed theoretically and empirically the exponential step size, a new step size decay schedule for the stochastic optimization of non-convex functions. This new step size is the continuous version of the stagewise step decay, a step size decay schedule widely used by practitioners. We have shown that, up to poly-logarithmic terms, this step size guarantees convergence with the best-known rates for smooth non-convex functions. Moreover, in the case of functions satisfying the PL condition, we have also proved that this step size is *adaptive* to the level of noise, without knowing it. Furthermore, we have validated our theoretical findings on both synthetic and real-world tasks, showing that this step size consistently matches or outperforms other step size decay schedules, while at the same time requiring only two hyperparameters to tune.

In future work, we plan to extend our theoretical results, both finding ways to weaken our assumptions and proving high probability bounds, thus strengthening our results in expectation.

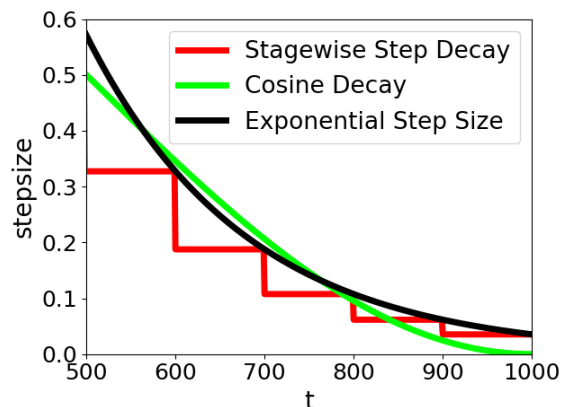


Figure 4: The step size decay curve of stagewise step decay, cosine decay, and ours.

Acknowledgements

This material is based upon work supported by the National Science Foundation under grant no. 1925930 “Collaborative Research: TRIPODS Institute for Optimization and Learning”.

References

- S. Arora, R. Ge, T. Ma, and A. Moitra. Simple, efficient, and neural algorithms for sparse coding. In Grnwald P, E. Hazan, and S. Kale, editors, *Proc. of The 28th Conference on Learning Theory*, volume 40 of *Proc. of Machine Learning Research*, pages 113–149, Paris, France, 03–06 Jul 2015. PMLR.
- N. S. Aybat, A. Fallah, M. Gurbuzbalaban, and A. Ozdaglar. A universally optimal multistage accelerated stochastic gradient method. In *Advances in Neural Information Processing Systems*, pages 8523–8534, 2019.
- F. Bach and E. Moulines. Non-asymptotic analysis of stochastic approximation algorithms for machine learning. In J. Shawe-Taylor, R. S. Zemel, P. L. Bartlett, F. Pereira, and K. Q. Weinberger, editors, *Advances in Neural Information Processing Systems 24*, pages 451–459. Curran Associates, Inc., 2011.
- L. Berrada, A. Zisserman, and M. Kumar. Deep frank-wolfe for neural network optimization. *International Conference on Learning Representations*, 2019.
- D. P. Bertsekas and J. N. Tsitsiklis. *Neuro-Dynamic Programming*. Athena Scientific, 1996.
- S. Bowman, G. Angeli, C. Potts, and C. Manning. A large annotated corpus for learning natural language inference. In *Proceedings of the 2015 Conference on Empirical Methods in Natural Language Processing (EMNLP)*. Association for Computational Linguistics, 2015.
- Y. Chen and E. Candes. Solving random quadratic systems of equations is nearly as easy as solving linear systems. In C. Cortes, N. D. Lawrence, D. D. Lee, M. Sugiyama, and R. Garnett, editors, *Advances in Neural Information Processing Systems 28*, pages 739–747. Curran Associates, Inc., 2015.
- A. Conneau, D. Kiela, H. Schwenk, L. Barrault, and A. Bordes. Supervised learning of universal sentence representations from natural language inference data. In *Proceedings of the 2017 Conference on Empirical*

- Methods in Natural Language Processing (EMNLP)*, pages 670–680, Copenhagen, Denmark, September 2017. Association for Computational Linguistics. URL <https://www.aclweb.org/anthology/D17-1070>.
- D. Davis, D. Drusvyatskiy, and V. Charisopoulos. Stochastic algorithms with geometric step decay converge linearly on sharp functions. *arXiv preprint arXiv:1907.09547*, 2019a.
- D. Davis, D. Drusvyatskiy, L. Xiao, and J. Zhang. From low probability to high confidence in stochastic convex optimization. *arXiv preprint arXiv:1907.13307*, 2019b.
- A. Defazio and L. Bottou. On the ineffectiveness of variance reduced optimization for deep learning. In *Advances in Neural Information Processing Systems*, pages 1753–1763, 2019.
- J. Duchi, E. Hazan, and Y. Singer. Adaptive subgradient methods for online learning and stochastic optimization. In *COLT*, 2010. URL https://stanford.edu/~jduchi/projects/DuchiHaSi10_colt.pdf.
- R. Ge, S. M. Kakade, R. Kidambi, and P. Netrapalli. The step decay schedule: A near optimal, geometrically decaying learning rate procedure for least squares. In *Advances in Neural Information Processing Systems*, pages 14951–14962, 2019.
- S. Ghadimi and G. Lan. Stochastic first-and zeroth-order methods for nonconvex stochastic programming. *SIAM Journal on Optimization*, 23(4):2341–2368, 2013.
- J.-L. Goffin. On convergence rates of subgradient optimization methods. *Mathematical programming*, 13(1): 329–347, 1977.
- E. Hazan and S. Kale. Beyond the regret minimization barrier: an optimal algorithm for stochastic strongly-convex optimization. In S. M. Kakade and U. von Luxburg, editors, *Proc. of the 24th Annual Conference on Learning Theory*, volume 19 of *Proc. of Machine Learning Research*, pages 421–436, Budapest, Hungary, 09–11 Jun 2011. PMLR.
- K. He, X. Zhang, S. Ren, and J. Sun. Deep residual learning for image recognition. In *Proc. of the IEEE conference on computer vision and pattern recognition*, pages 770–778, 2016.
- T. He, Z. Zhang, H. Zhang, Z. Zhang, J. Xie, and M. Li. Bag of tricks for image classification with convolutional neural networks. In *The IEEE Conference on Computer Vision and Pattern Recognition (CVPR)*, June 2019.
- G. Huang, Z. Liu, L. Van Der Maaten, and K. Q. Weinberger. Densely connected convolutional networks. In *Proceedings of the IEEE conference on Computer Vision and Pattern Recognition*, pages 4700–4708, 2017.
- C. Jin, R. Ge, P. Netrapalli, S.M. Kakade, and M. I. Jordan. How to escape saddle points efficiently. In *Proc. of the 34th International Conference on Machine Learning*, volume 70, pages 1724–1732. PMLR, 2017.
- H. Karimi, J. Nutini, and M. Schmidt. Linear convergence of gradient and proximal-gradient methods under the Polyak-Łojasiewicz condition. In *Joint European Conference on Machine Learning and Knowledge Discovery in Databases*, pages 795–811. Springer, 2016.
- A. Khaled and P. Richtárik. Better theory for SGD in the nonconvex world. *arXiv preprint arXiv:2002.03329*, 2020.
- D. P. Kingma and J. Ba. Adam: A method for stochastic optimization. In *International Conference on Learning Representations (ICLR)*, 2015.
- B. Kleinberg, Y. Li, and Y. Yuan. An alternative view: When does SGD escape local minima? In J. Dy and A. Krause, editors, *Proc. of the 35th International Conference on Machine Learning*, volume 80 of *Proc. of Machine Learning Research*, pages 2698–2707, Stockholmsmssan, Stockholm Sweden, 10–15 Jul 2018. PMLR.
- A. Krizhevsky, I. Sutskever, and G. E. Hinton. Imagenet classification with deep convolutional neural networks. In *Advances in Neural Information Processing Systems*, pages 1097–1105, 2012.

- A. Kulunchakov and J. Mairal. A generic acceleration framework for stochastic composite optimization. In *Advances in Neural Information Processing Systems*, pages 12556–12567, 2019.
- C. Lee, S. Xie, P. Gallagher, Z. Zhang, and Z. Tu. Deeply-supervised nets. In *Proc. of the Eighteenth International Conference on Artificial Intelligence and Statistics*, volume 38, pages 562–570. PMLR, 2015.
- L. Lei, C. Ju, J. Chen, and M. I. Jordan. Non-convex finite-sum optimization via SCSG methods. In *Advances in Neural Information Processing Systems 30*, pages 2348–2358. Curran Associates, Inc., 2017.
- Y. Li and Y. Yuan. Convergence analysis of two-layer neural networks with ReLU activation. In I. Guyon, U. V. Luxburg, S. Bengio, H. Wallach, R. Fergus, S. Vishwanathan, and R. Garnett, editors, *Advances in Neural Information Processing Systems 30*, pages 597–607. Curran Associates, Inc., 2017.
- Z. Li and S. Arora. An exponential learning rate schedule for deep learning. In *8th International Conference on Learning Representations, ICLR 2020, Addis Ababa, Ethiopia, April 26-30, 2020*. OpenReview.net, 2020.
- S. Lojasiewicz. A topological property of real analytic subsets (in french). *Coll. du CNRS, Les équations aux dérivées partielles*, pages 87–89, 1963.
- I. Loshchilov and F. Hutter. Large batch optimization for deep learning: Training BERT in 76 minutes. In *International Conference on Learning Representations*, 2017.
- H. B. McMahan and M. J. Streeter. Adaptive bound optimization for online convex optimization. In *COLT*, 2010. URL <https://static.googleusercontent.com/media/research.google.com/en//pubs/archive/36483.pdf>.
- Y. Nesterov. A method for unconstrained convex minimization problem with the rate of convergence $O(1/k^2)$. In *Doklady AN SSSR (translated as Soviet. Math. Doct.)*, volume 269, pages 543–547, 1983.
- Y. Nesterov. *Introductory lectures on convex optimization: A basic course*, volume 87. Springer, 2004.
- J. Pennington, R. Socher, and C. Manning. Glove: Global vectors for word representation. In *Proceedings of the 2014 Conference on Empirical Methods in Natural Language Processing (EMNLP)*, pages 1532–1543, 2014.
- B. T. Polyak. Gradient methods for minimizing functionals. *Zhurnal Vychislitel’noi Matematiki i Matematicheskoi Fiziki*, 3(4):643–653, 1963.
- S. J. Reddi, A. Hefny, S. Sra, B. Póczos, and A. Smola. Stochastic variance reduction for nonconvex optimization. In *International conference on machine learning*, pages 314–323, 2016.
- S. J. Reddi, S. Kale, and S. Kumar. On the convergence of Adam and beyond. In *International Conference on Learning Representations*, 2018. URL <https://openreview.net/pdf?id=ryQu7f-RZ>.
- H. Robbins and S. Monro. A stochastic approximation method. *Annals of Mathematical Statistics*, 22: 400–407, 1951.
- K. Simonyan and A. Zisserman. Very deep convolutional networks for large-scale image recognition. In *Proc. of the International Conference on Learning Representations (ICLR)*, 2015.
- R. Sun and Z. Luo. Guaranteed matrix completion via non-convex factorization. *IEEE Transactions on Information Theory*, 62(11):6535–6579, 2016.
- T. Tieleman and G. Hinton. Lecture 6.5-rmsprop: Divide the gradient by a running average of its recent magnitude. *COURSERA: Neural Networks for Machine Learning*, 2012.
- S. Vaswani, F. Bach, and M. Schmidt. Fast and faster convergence of SGD for over-parameterized models and an accelerated Perceptron. In K. Chaudhuri and M. Sugiyama, editors, *Proc. of the 22nd International Conference on Artificial Intelligence and Statistics*, volume 89 of *Proc. of Machine Learning Research*, pages 1195–1204. PMLR, 16–18 Apr 2019a.

- S. Vaswani, A. Mishkin, I. Laradji, M. Schmidt, G. Gidel, and S. Lacoste-Julien. Painless stochastic gradient: Interpolation, line-search, and convergence rates. In *Advances in Neural Information Processing Systems*, pages 3727–3740, 2019b.
- Y. Xu, Q. Lin, and T. Yang. Accelerated stochastic subgradient methods under local error bound condition. *arXiv preprint arXiv:1607.01027*, 2016.
- Z. Yuan, Y. Yan, R. Jin, and T. Yang. Stagewise training accelerates convergence of testing error over sgd. In *Advances in Neural Information Processing Systems*, pages 2604–2614, 2019.
- M. D. Zeiler. ADADELTA: an adaptive learning rate method. *arXiv preprint arXiv:1212.5701*, 2012.
- H. Zhang and W. Yin. Gradient methods for convex minimization: better rates under weaker conditions. *arXiv preprint arXiv:1303.4645*, 2013.
- Z. Zhang, Y. Wu, and G. Wang. Bpgrad: Towards global optimality in deep learning via branch and pruning. In *Proceedings of the IEEE Conference on Computer Vision and Pattern Recognition*, pages 3301–3309, 2018.
- Z. Zhou, P. Mertikopoulos, N. Bambos, S. Boyd, and P. W. Glynn. Stochastic mirror descent in variationally coherent optimization problems. In *Advances in Neural Information Processing Systems*, pages 7043–7052, 2017.
- A. Z. Zhu. How to make the gradients small stochastically: Even faster convex and nonconvex SGD. In *Advances in Neural Information Processing Systems 31*, pages 1157–1167, 2018a.
- Z. Zhu. Natasha 2: Faster non-convex optimization than SGD. In S. Bengio, H. Wallach, H. Larochelle, K. Grauman, N. Cesa-Bianchi, and R. Garnett, editors, *Advances in Neural Information Processing Systems 31*, pages 2675–2686. Curran Associates, Inc., 2018b.

A Appendix

A.1 Convergence for non-Lipschitz PL functions

Karimi et al. [2016] proved that SGD with an appropriate step size will give a $O(1/T)$ convergence for Lipschitz and PL functions. However, it is easy to see that the Lipschitz assumption can be substituted by the smoothness one and obtain a rate that depends on the variance of the noise. Even if this is a straightforward result, we could not find it anywhere so we report here our proof.

Theorem 3. *Assume (A1) and (A3) and set the step sizes $\eta_t = \min\left(\frac{1}{L(1+a)}, \frac{2t+1}{\mu(t+1)^2}\right)$. Then, SGD guarantees*

$$f(\mathbf{x}_{T+1}) - f^* \leq \frac{L^2(1+a)b}{2\mu^3T^2} + \frac{2L}{\mu^2T}b + (f(\mathbf{x}_1) - f^*) \frac{L^2(1+a)^2}{\mu^2T^2} \left(1 - \frac{\mu}{L(1+a)}\right)^{\frac{L(1+a)}{\mu}}.$$

Proof. For simplicity, denote $\mathbb{E}f(\mathbf{x}_t) - f^*$ by Δ_t . With the same analysis as in Theorem 1, we have

$$\Delta_{t+1} \leq (1 - \mu\eta_t) \Delta_t + \frac{L}{2}\eta_t^2b.$$

Denote by $t^* = \min\left\{t : \frac{t^2}{2t+1} \leq \frac{L(1+a)-\mu}{\mu}\right\}$. When $t \leq t^*$, $\eta_t = \frac{1}{L(1+a)}$ and we obtain

$$\Delta_{t+1} \leq \left(1 - \frac{\mu}{L(1+a)}\right) \Delta_t + \frac{b}{2L(1+a)^2}.$$

Thus, by Lemma 1, we get

$$\begin{aligned} \Delta_{t^*} &\leq \left(1 - \frac{\mu}{L(1+a)}\right)^{t^*-1} \Delta_1 + \frac{b}{2L(1+a)^2} \sum_{i=0}^{t^*-1} \left(1 - \frac{\mu}{L(1+a)}\right)^{t^*-i} \\ &\leq \left(1 - \frac{\mu}{L(1+a)}\right)^{t^*} \Delta_1 + \frac{b}{2\mu(1+a)}. \end{aligned}$$

Instead, when $t \geq t^*$, $\eta_t = \frac{2t+1}{\mu(t+1)^2}$, we have

$$\Delta_{t+1} \leq \frac{t^2}{(t+1)^2} \Delta_t + \frac{L(2t+1)^2}{2\mu^2(t+1)^4} b.$$

Multiplying both sides by $(t+1)^2$ and denoting by $\delta_t = t^2\Delta_t$, we get

$$\delta_{t+1} \leq \delta_t + \frac{L(2t+1)^2}{2\mu^2(t+1)^2} b \leq \delta_t + \frac{2L}{\mu^2} b.$$

Summing over t from t^* to T , we have

$$\delta_{T+1} \leq \delta_{t^*} + \frac{2L(T-t^*)}{\mu^2} b.$$

Then, we finally get

$$\begin{aligned} \Delta_{T+1} &\leq \frac{t^{*2}}{T^2} \left(1 - \frac{\mu}{L(1+a)}\right)^{t^*} \Delta_1 + \frac{t^{*2}b}{2\mu(1+a)T^2} + \frac{2L(T-t^*)}{\mu^2T^2} b \\ &\leq \frac{L^2(1+a)^2}{\mu^2T^2} \left(1 - \frac{\mu}{L(1+a)}\right)^{\frac{L(1+a)}{\mu}} \Delta_1 + \frac{L^2(1+a)b}{2\mu^3T^2} + \frac{2L}{\mu^2T} b. \end{aligned} \quad \square$$

A.2 Proofs in Section 4

Proof of Lemma 1. When $k = 1$, $X_2 \leq A_1 X_1 + B_1$ satisfies. By induction, assume $X_k \leq \prod_{i=1}^{k-1} A_i X_1 + \sum_{i=1}^{k-1} \prod_{j=i+1}^{k-1} A_j B_i$, and we have

$$\begin{aligned} X_{k+1} &\leq A_k \left(\prod_{i=1}^{k-1} A_i X_1 + \sum_{i=1}^{k-1} \prod_{j=i+1}^{k-1} A_j B_i \right) + B_k \\ &= \prod_{i=1}^k A_i X_1 + \sum_{i=1}^{k-1} \prod_{j=i+1}^k A_j B_i + A_k B_k \\ &= \prod_{i=1}^k A_i X_1 + \sum_{i=1}^k \prod_{j=i+1}^k A_j B_i. \end{aligned} \quad \square$$

Proof of Lemma 2. We have

$$\begin{aligned} \exp\left(\frac{\mu\alpha^{T+1}}{L(1+a)(1-\alpha)}\right) &= \exp\left(\frac{\mu\alpha\beta}{TL(1+a)(1-\alpha)}\right) \\ &\leq \exp\left(\frac{\mu\beta}{TL(1+a)(1-\alpha)}\right) = \exp\left(\frac{\mu\beta}{TL(1+a)\left(1 - \exp\left(-\frac{1}{T} \ln \frac{T}{\beta}\right)\right)}\right) \\ &\leq \exp\left(\frac{2\mu\beta}{L(1+a) \ln \frac{T}{\beta}}\right) = C(\beta), \end{aligned}$$

where in the last inequality we used $\exp(-x) \leq 1 - \frac{x}{2}$ for $0 < x < \frac{1}{e}$ and the fact that $\frac{1}{T} \ln\left(\frac{T}{\beta}\right) \leq \frac{\ln T}{T} \leq \frac{1}{e}$. \square

Proof of Lemma 3. It is enough to prove that $f(x) := x - 1 - \ln x \geq 0$. Observe that $f'(x)$ is increasing and $f'(1) = 0$, hence, we have $f(x) \geq f(1) = 0$. \square

A.3 Experiments details

A.3.1 Synthetic Experiments

We conduct an experiment on a non-convex function $g(r, \theta) = (2 + \frac{\cos \theta}{2} + \cos 4\theta)r^2(5/3 - r)$ [Zhou et al., 2017], where r and θ are the polar coordinates, which satisfies the PL condition when $r \leq 1$. We compare SGD with decay rules listed in (4), SGD with a constant step size, and Adam on optimizing this function. We consider three cases: the noiseless case where we get the exact gradient in each round, the slightly noisy case in which we add independent Gaussian noise with zero mean and standard deviation 0.05 to each dimension of the gradient in each round, and the noisy case with additive Gaussian noise of standard deviation 1. For the noiseless case, we run 50 iterations and report the best one as we are already very close to the optimum; whereas for the noisy case, we run 200 iterations and report the results of the best hyperparameter setting for each method averaged on 20 independent runs with different random seeds. Results shown in Figure 5 demonstrate that our scheme behaves as the theory predicts and is the best in all cases.

Proof of PL condition. We now prove that $f(x, y) = g(r, \theta) = (2 + \frac{\cos \theta}{2} + \cos 4\theta)r^2(5/3 - r)$ satisfies the PL condition when $r \leq 1$.

Obviously, $2 + \frac{\cos \theta}{2} + \cos 4\theta \geq \frac{1}{2}$ as $\cos \theta \in [-1, 1]$.

When $r \leq 1$, $\frac{5}{3} - r \geq \frac{2}{3}$, thus $f(x, y) \geq 0$, and $f^* = f(0, 0) = 0$.

We first calculate derivatives in polar coordinates

$$\begin{aligned} \frac{\partial g}{\partial r} &= \left(\frac{10r}{3} - 3r^2\right) \left(2 + \frac{\cos \theta}{2} + \cos 4\theta\right), \\ \frac{\partial g}{\partial \theta} &= \left(-\frac{\sin \theta}{2} - 4 \sin 4\theta\right) r^2 \left(\frac{5}{3} - r\right). \end{aligned}$$

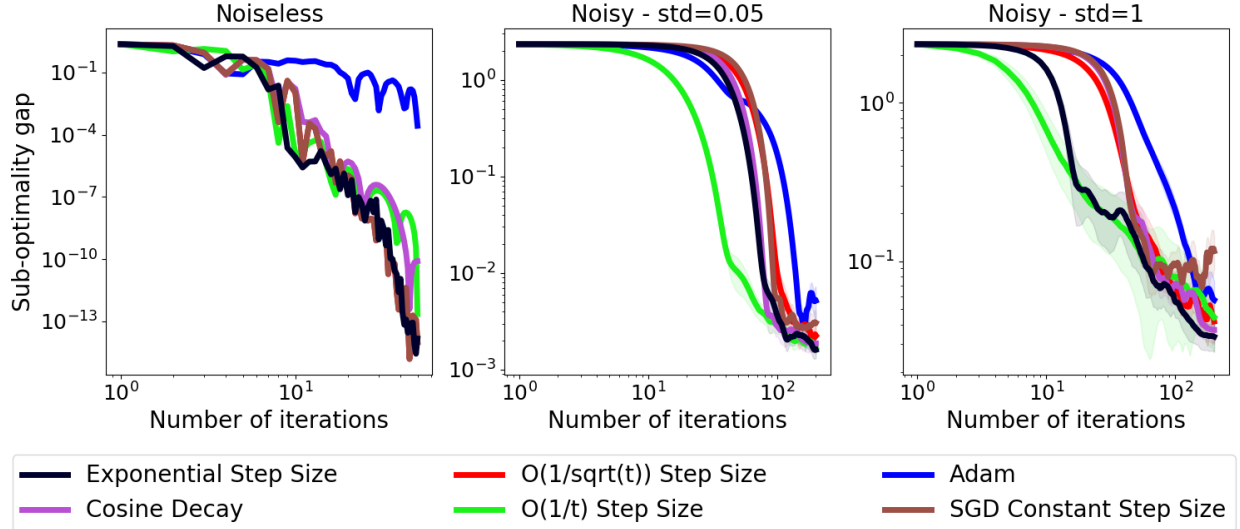


Figure 5: Plots of the sub-optimality gap vs. iterations for optimizing a synthetic function. Both axes in all figures are in logarithmic scale. The left plot is the noiseless case, the middle one is with the additive Gaussian noise of standard deviation 0.05, while the right plot is with the additive Gaussian noise of standard deviation 1.

Then, from the relationship between derivatives in Cartesian and polar coordinates, we have

$$\begin{aligned}
 \frac{\|\nabla f(x, y)\|^2}{2(f(x, y) - f^*)} &= \frac{\left(\frac{\partial g}{\partial r}\right)^2 + \frac{1}{r^2} \left(\frac{\partial g}{\partial \theta}\right)^2}{2\left(2 + \frac{\cos \theta}{2} + \cos 4\theta\right)r^2\left(\frac{5}{3} - r\right)} \\
 &= \frac{\left(\frac{10}{3} - 3r\right)^2\left(2 + \frac{\cos \theta}{2} + \cos 4\theta\right)}{\frac{10}{3} - 2r} + \frac{\left(-\frac{\sin \theta}{2} - 4 \sin 4\theta\right)^2\left(\frac{5}{3} - r\right)}{2\left(2 + \frac{\cos \theta}{2} + \cos 4\theta\right)} \\
 &\geq \frac{\left(\frac{10}{3} - 3r\right)^2}{4\left(\frac{5}{3} - r\right)} \geq \frac{1}{24}.
 \end{aligned}$$

Hyperparameter tuning. We tune each method using a two-stage grid search. Note that for Adam, we fix $\beta_1 = 0.9$ and $\beta_2 = 0.999$ following Kingma and Ba [2015]. The first (coarse) searching grid of the starting step size is $\{0.0001, 0.001, 0.01, 0.1, 1, 10\}$, while the second (fine) searching grid will be, for example, $\{0.001, 0.003, 0.005, 0.007, 0.009, 0.01, 0.03, 0.05, 0.07, 0.09\}$ if the best starting step size in the first stage is 0.01. For the α value, as its effect is reflected on the ratio η_T/η_0 where η_T is the step size in the last iteration, we set the searching grid of α so that the respective searching grid for η_T/η_0 is first (coarse) $\{0.0001, 0.001, 0.01, 0.1, 1\}$ and then (fine) $\{0.001, 0.003, 0.005, 0.007, 0.009, 0.01, 0.03, 0.05, 0.07, 0.09\}$ if the best η_T/η_0 in the first stage is 0.01. Note that we try all pairs of (η_0, α) from their respective searching grids. Moreover, whenever the best run lie in the boundary of the grid, we extend the grid to make the best hyperparameter be contained in the interior of the grid.

A.3.2 Image classification experiments.

Data Normalization and Augmentation. Images are normalized per channel using the means and standard deviations computed from all training images. For CIFAR-10/100, we adopt the data augmentation technique following Lee et al. [2015] (for training only): 4 pixels are padded on each side of an image and a 32×32 crop is randomly sampled from the padded image or its horizontal flip.

Hyperparameter tuning. We tune the hyperparameters on the validation set using the following two-stage grid searching strategy. First, search over a coarse grid, and select the one yielding the best validation

results. Next, continue searching in a fine grid centering at the best performing hyperparameters found in the coarse stage, and in turn take the best one as the final choice.

For the starting step size η_0 , the coarse searching grid is $\{0.00001, 0.0001, 0.001, 0.01, 0.1, 1\}$, and the fine grid is like $\{0.006, 0.008, 0.01, 0.02, 0.04\}$ if the best one in the coarse stage is 0.01.

For the α value, we set its searching grid so that the ratio η_T/η_0 , where η_T is the step size in the last iteration, is first searched over the coarse grid of $\{0.00001, 0.0001, 0.001, 0.01, 0.1, 1\}$, and then over a fine grid centered at the best one of the coarse stage. Note that we try all pairs of (η_0, α) from their respective searching grids.

For the stagewise step decay, to make the tuning process more thorough, we modify as follows the one employed in Section 6.1 (specifically on tuning SGD V1) of Yuan et al. [2019], where they first set two milestones and then tune the starting step size. Put it explicitly and take the experiment on CIFAR-10 as an example, we first run vanilla SGD with a constant step size to search for a good range of starting step size on grid $\{0.00001, 0.0001, 0.001, 0.01, 0.1, 1\}$, and find 0.01 and 0.1 work well. Based on this, we set the fine searching grid of starting step sizes as $\{0.007, 0.01, 0.04, 0.07, 0.1, 0.4\}$. For each of them, we run three settings with increasing number of milestones: vanilla SGD (with no milestone), SGD with 1 milestone, and SGD with 2 milestones. The searching grid for milestones is $\{16k, 24k, 32k, 40k, 48k, 56k\}$ (number of iterations). For the 1 milestone setting, the milestone can be any of them. For the 2 milestones, they can be any combination of two different elements from the searching grid, like (16k, 32k) or (32k, 48k). The grid search strategy for FashionMNIST and CIFAR-100 is similar but with the searching grid for milestones over $\{3k, 6k, 9k, 12k, 15k, 18k\}$.

The PyTorch ReduceLRonPlateau scheduler takes multiple arguments, among which we tune the starting learning rate, the factor argument which decides by which the learning rate will be reduced, the patience argument which controls the number of epochs with no improvement after which learning rate will be reduced, and the threshold argument which measures the new optimum to only focus on significant changes. We choose the searching grid for the starting step size using the same strategy for stagewise step decay above, i.e., first run SGD with a constant step size to search for a good starting step size, then search over a grid centering on the found value, which results in the grid $\{0.004, 0.007, 0.01, 0.04, 0.07\}$ (FashionMNIST) and $\{0.01, 0.04, 0.07, 0.1, 0.4\}$ (CIFAR10/100). We also explore the searching grid of the factor argument over $\{0.1, 0.5\}$, the patience argument over $\{5, 10\}$ (CIFAR10) or $\{3, 6\}$ (FashionMNIST/CIFAR100), and the threshold argument over $\{0.0001, 0.001, 0.01, 0.1\}$.

For each setting, we choose the combination of hyperparameters that gives the best final validation loss to be used in the testing stage. Also, whenever the best performing hyperparameters lie in the boundary of the searching grid, we always extend the grid to make the final best performing hyperparameters fall into the interior of the grid.

Detailed final Results In Table 1 we show the specific result numbers of each experiment.

Table 1: The average final training loss and test accuracy achieved by each method when optimizing respective models on each dataset. The \pm shows 95% confidence intervals of the mean loss/accuracy value over 5 runs starting from different random seeds.

Methods	FashionMNIST		CIFAR10		CIFAR100	
	Training loss	Test accuracy	Training loss	Test accuracy	Training loss	Test accuracy
SGD Constant Step Size	0.0068 \pm 0.0023	0.9297 \pm 0.0033	0.2226 \pm 0.0169	0.8674 \pm 0.0048	1.1467 \pm 0.1437	0.5896 \pm 0.0404
$O(1/t)$ Step Size	0.0013 \pm 0.0004	0.9297 \pm 0.0021	0.0331 \pm 0.0028	0.8894 \pm 0.0040	0.3489 \pm 0.0263	0.6874 \pm 0.0076
$O(1/\sqrt{t})$ Step Size	0.0016 \pm 0.0005	0.9262 \pm 0.0014	0.0672 \pm 0.0086	0.8814 \pm 0.0034	0.8147 \pm 0.0717	0.6336 \pm 0.0169
Cosine Decay	0.0004 \pm 0.0000	0.9285 \pm 0.0019	0.0106 \pm 0.0008	0.9199 \pm 0.0029	0.0949 \pm 0.0053	0.7497 \pm 0.0044
Adam	0.0203 \pm 0.0021	0.9168 \pm 0.0023	0.1161 \pm 0.0111	0.8823 \pm 0.0041	0.6513 \pm 0.0154	0.6478 \pm 0.0054
SGD+Armijo	0.0003 \pm 0.0000	0.9284 \pm 0.0016	0.0185 \pm 0.0043	0.8973 \pm 0.0071	0.1063 \pm 0.0153	0.6768 \pm 0.0044
ReduceLRonPlateau	0.0031 \pm 0.0009	0.9294 \pm 0.0015	0.0867 \pm 0.0230	0.9033 \pm 0.0049	0.0927 \pm 0.0085	0.7435 \pm 0.0076
Stagewise - 1 Milestone	0.0007 \pm 0.0002	0.9294 \pm 0.0018	0.0269 \pm 0.0017	0.9062 \pm 0.0020	0.2673 \pm 0.0084	0.7459 \pm 0.0030
Stagewise - 2 Milestones	0.0023 \pm 0.0005	0.9283 \pm 0.0024	0.0322 \pm 0.0008	0.9174 \pm 0.0020	0.1783 \pm 0.0030	0.7487 \pm 0.0025
Exponential Step Size	0.0006 \pm 0.0001	0.9290 \pm 0.0009	0.0098 \pm 0.0010	0.9188 \pm 0.0033	0.0714 \pm 0.0041	0.7398 \pm 0.0037

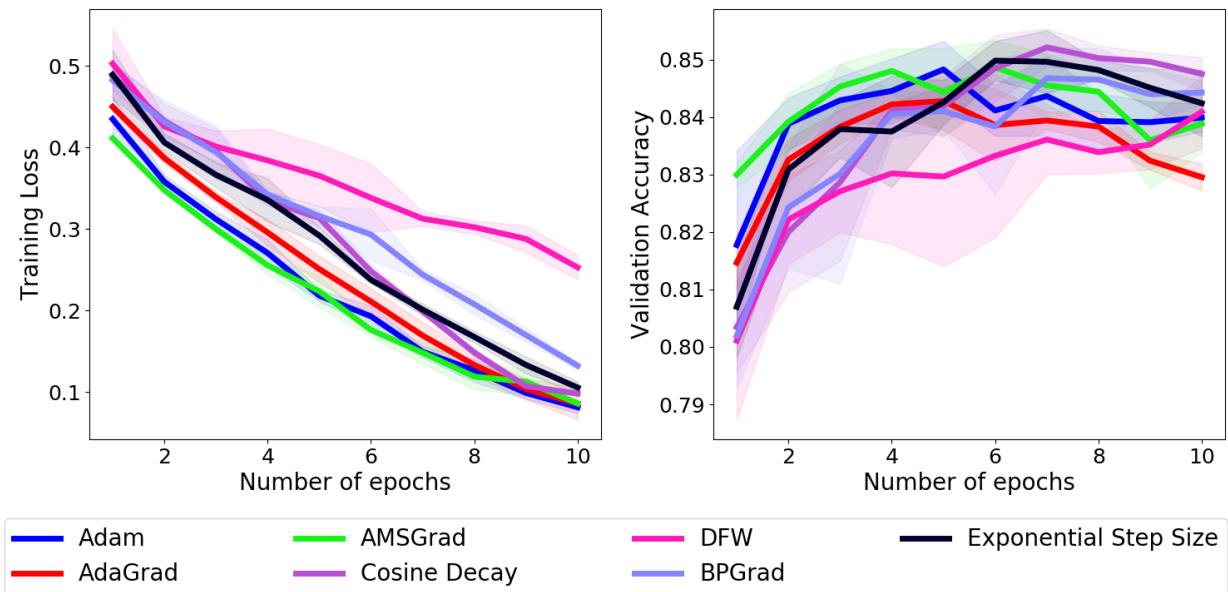


Figure 6: Training loss and validation accuracy curves, averaged over 5 independent runs, on using different methods to optimize a Bi-LSTM to do natural language inference on the SNLI dataset.

A.3.3 Natural language inference

Dataset We conduct this experiment on the Stanford Natural Language Inference (SNLI) dataset [Bowman et al., 2015], which contains 570k pairs of human-generated English sentences. Each pair of sentences is manually labeled with one of three categories: entailment, contradiction, and neutral, and thus forms a three-way classification problem. It captures the task of natural language inference, also known as Recognizing Textual Entailment (RTE).

Model We employ the bi-directional LSTM of about 47M parameters proposed by Conneau et al. [2017]. Except for replacing the cross-entropy loss with an SVM loss following Berrada et al. [2019], we leave all other components unchanged (codes can be found here⁶). Like them, we also use the open-source GloVe vectors [Pennington et al., 2014] trained on Common Crawl 840B with 300 dimensions as fixed word embeddings.

Training During the validation stage, we tune each method using the grid search. The initial learning rate of each method is grid searched over $\{0.00001, 0.0001, 0.001, 0.01, 0.1, 1, 10\}$. And the α of our exponential step size is searched over a grid such that the ratio η_T/η_0 , where η_T is the step size in the last iteration, is over $\{0.0001, 0.001, 0.01, 0.1, 1\}$. Following [Berrada et al., 2019], for each hyperparameter setting, we record the best validation accuracy obtained during training, and select the setting that performs the best according to this metric to do the test. The testing stage is repeated with different random seeds for 5 times to eliminate the influence of stochasticity.

We employ the Nesterov momentum [Nesterov, 1983] of 0.9 without dampening (if having this option), but do not use weight decay. The mini-batch size is 64 and we run for 10 epochs.

Results We compare our exponential step size with Adagrad, Adam, AMSGrad [Reddi et al., 2018], BPGGrad [Zhang et al., 2018], DFW [Berrada et al., 2019], and Cosine decay. From Figure 6 and Table 2, we can see that cosine decay remains the best among all methods, but our exponential step size can still match its performance and outperform all the other methods.

⁶<https://github.com/oval-group/dfw>

Table 2: The best test accuracy achieved by each method. The \pm shows 95% confidence intervals of the mean accuracy value over 5 runs starting from different random seeds.

Methods	Test Accuracy
Adam	0.8479 ± 0.0043
AdaGrad	0.8446 ± 0.0027
AMSGrad	0.8475 ± 0.0029
DFW	0.8412 ± 0.0045
BPGgrad	0.8459 ± 0.0030
Cosine Decay	0.8509 ± 0.0033
Exp. Step Size	0.8502 ± 0.0028